Electronic Supplementary Material (ESI) for New Journal of Chemistry.

Electronic Supplementary Information

Tetrakis-(N-methyl-4-pyridinium)-Porphyrin as a Diamagnetic Chemical Exchange Saturation Transfer (diaCEST) MRI Contrast Agent

Subhayan Chakraborty[a], Mainak Das[a], A. Srinivasan*[a] and Arindam Ghosh*[a]

[a] School of Chemical Sciences, National Institute of Science Education and Research (HBNI), At/PO Jatni, Khurdha 752050

*Corresponding authors: srini@niser.ac.in (AS), aringh@niser.ac.in (AG)

Table of contents

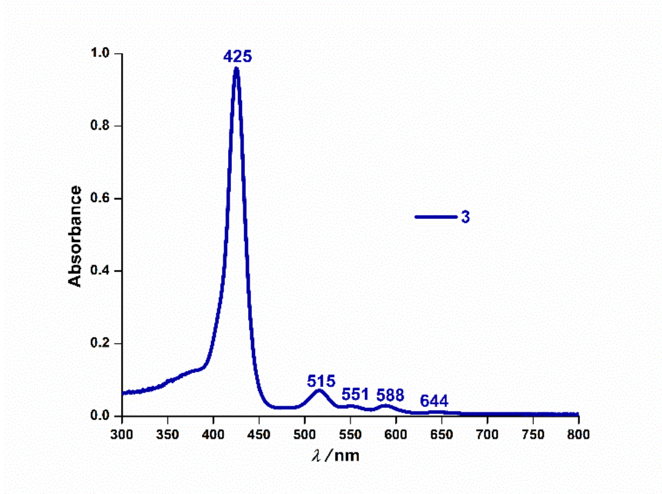

Figure S1: UV absorption spectrum of **TmPyP** (please refer to compound **2** in Chart 1 in the manuscript for the structure) in DMSO. The characteristic sharp soret band appears at 425 nm along with four weak Q bands at 515nm, 551nm, 588nm and 644nm.

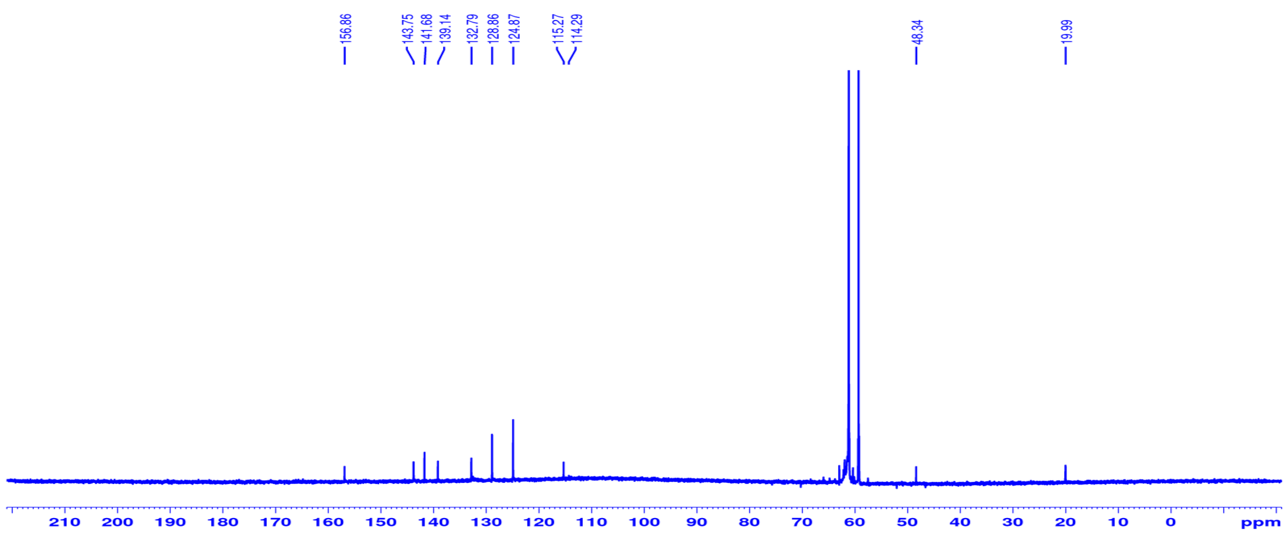

Figure S2: ^{13}C-NMR spectrum of **TmPyP** in DMSO-d_6 recorded on 700 MHz. δ 19.99, 48.34, 114.29, 115.27, 124.87, 128.86, 132.79, 139.14, 141.68, 143.75 and 156.86.

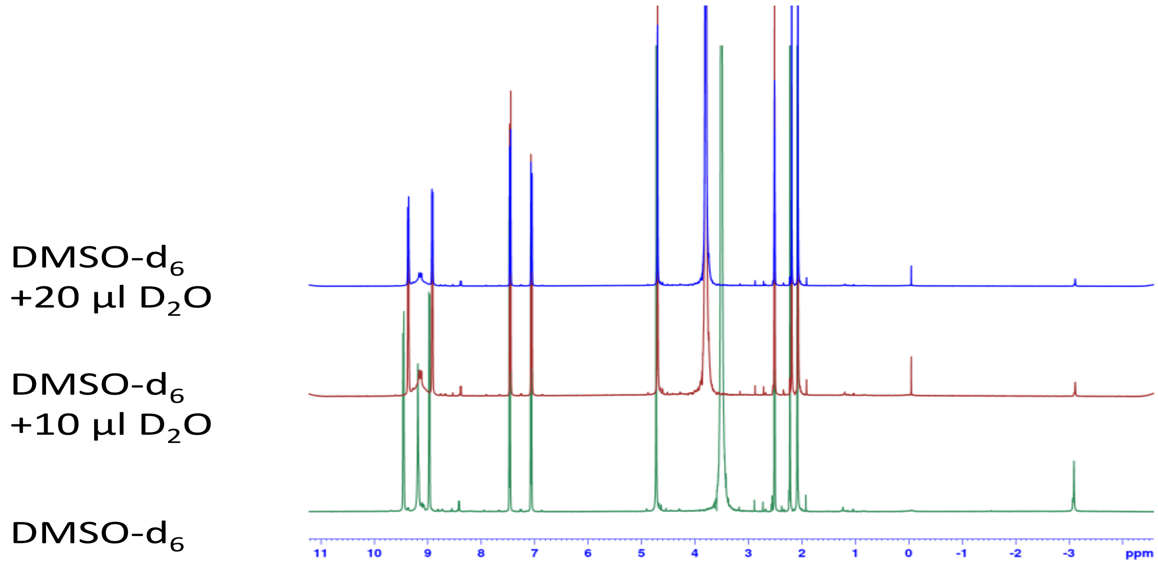

Figure S3: 1H NMR of **TmPyP** in DMSO-d_6. The inner core amine NH proton resonates at -3 ppm. Upon addition of 10µl of D_2O the intensity of this proton reduces and almost vanishes after the addition of another 10µl of D_2O. This shows the exchangeable behavior of this inner core NH protons that are highly upfield shifted.

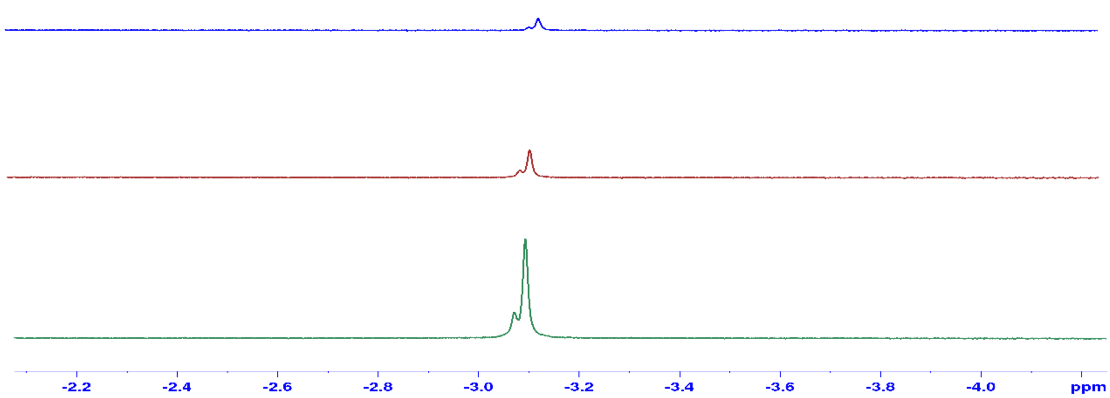

Figure S4: Expanded region around –3 ppm of the spectra shown in Figure S5 indicating the decrease in intensity of the exchangeable proton upon addition of 10 µl and 20 µl of D_2O.

a. b.

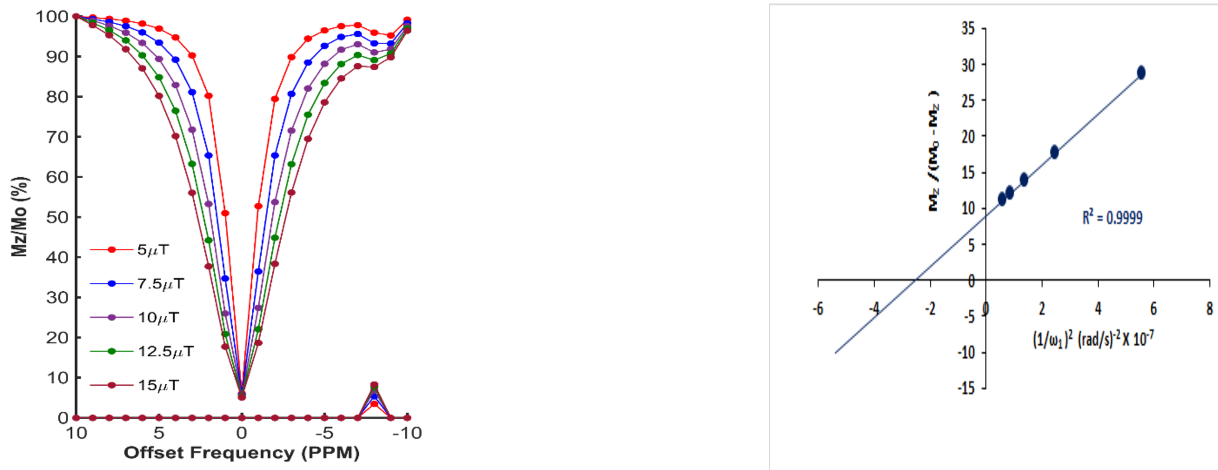

Figure S5 : (a) Dependence of CEST percentage on saturation field strength ranging from 5μT to 15μT for pH 6.6 (b) Omega plot for exchange rate measurement. The expected linear relationship of $M_z/(M_0\text{-}M_z)$ as a function of $1/\omega_1^2$ (rad/sec)$^{-2}$ x 10^{-7} recorded at 9.4 T of 12.5 mM compound in 0.1M Tris-HCl buffer at pH 6.6. RF saturation pulse was applied for 6 s ensuring complete saturation.

a. b.

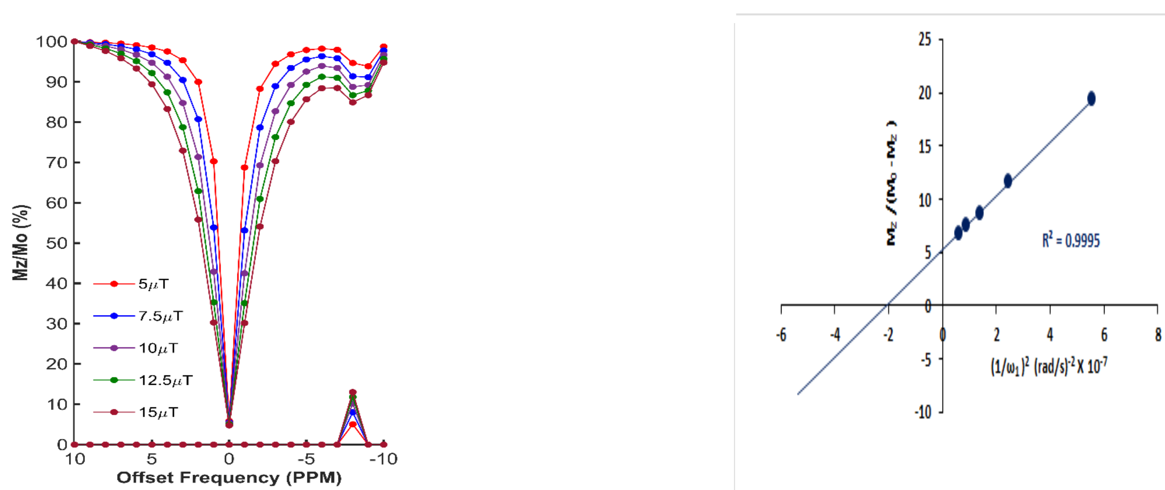

Figure S6: (a) Dependence of CEST percentage on saturation field strength ranging from 5μT to 15μT for pH 7.0 (b) Omega plot for exchange rate measurement. The expected linear relationship of $M_z/(M_0\text{-}M_z)$ as a function of $1/\omega_1^2$ (rad/sec)$^{-2}$ x 10^{-7} recorded at 9.4 T of 12.5 mM compound in 0.1M Tris-HCl buffer at pH 7.0. RF saturation pulse was applied for 6 s ensuring complete saturation.

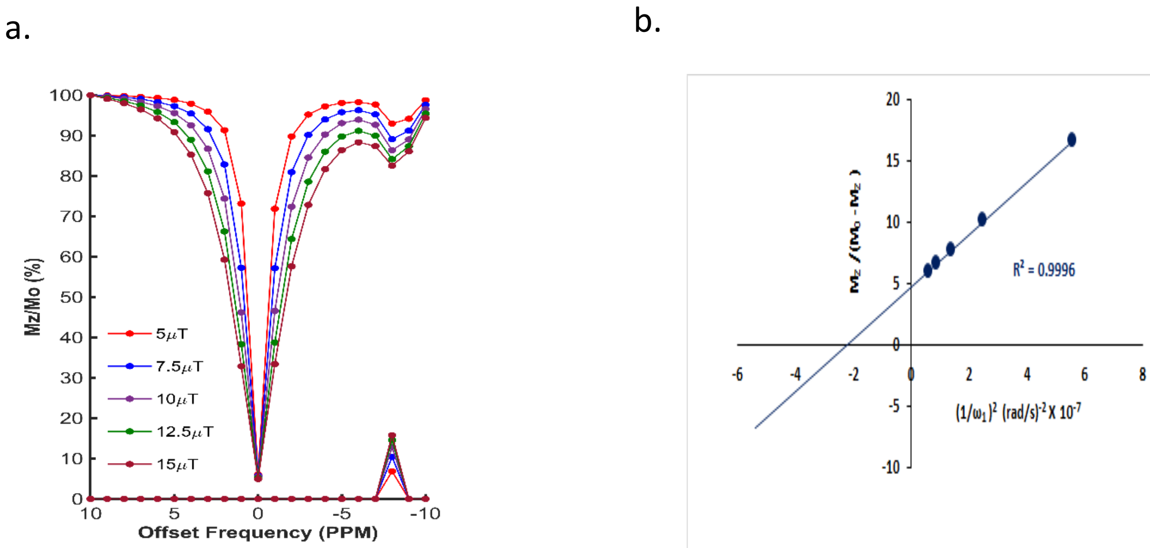

Figure S7: (a) Dependence of CEST percentage on saturation field strength ranging from 5μT to 15μT for pH 7.2 (b) Omega plot for exchange rate measurement. The expected linear relationship of $M_z/(M_0-M_z)$ as a function of $1/\omega_1^2$ (rad/sec)$^{-2}$ x 10^{-7} recorded at 9.4 T of 12.5 mM compound in 0.1M Tris-HCl buffer at pH 7.2. RF saturation pulse was applied for 6 s ensuring complete saturation.

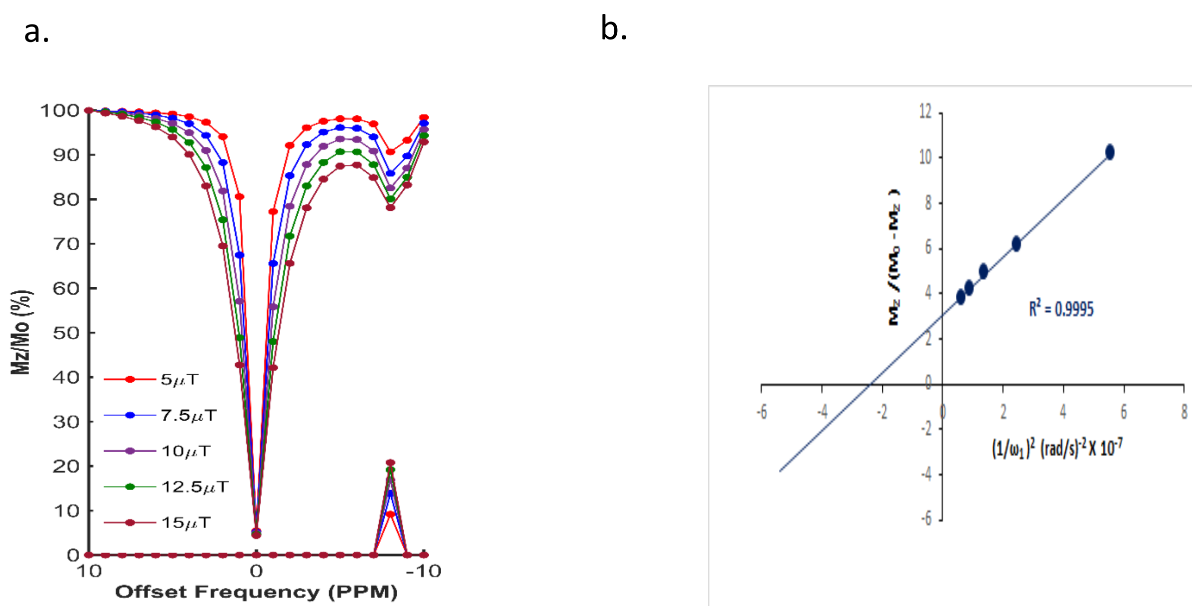

Figure S8: (a) Dependence of CEST percentage on saturation field strength ranging from 5μT to 15μT for pH 7.6 (b) Omega plot for exchange rate measurement. The expected linear relationship of $M_z/(M_0-M_z)$ as a function of $1/\omega_1^2$ (rad/sec)$^{-2}$ x 10^{-7} recorded at 9.4 T of 12.5 mM compound in 0.1M Tris-HCl buffer at pH 7.6. RF saturation pulse was applied for 6 s ensuring complete saturation.

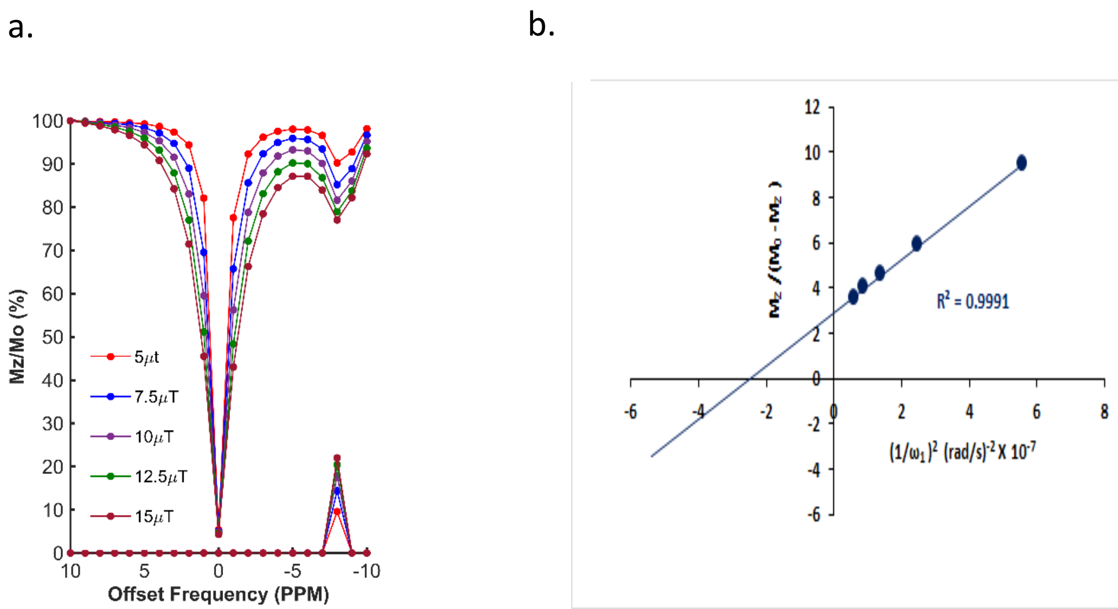

Figure S9: (a) Dependence of CEST percentage on saturation field strength ranging from 5μT to 15μT for pH 7.8 (b) Omega plot for exchange rate measurement. The expected linear relationship of $M_z/(M_0-M_z)$ as a function of $1/\omega_1^2$ (rad/sec)$^{-2}$ x 10^{-7} recorded at 9.4 T of 12.5 mM compound in 0.1M Tris-HCl buffer at pH 7.8. RF saturation pulse was applied for 6 s ensuring complete saturation.

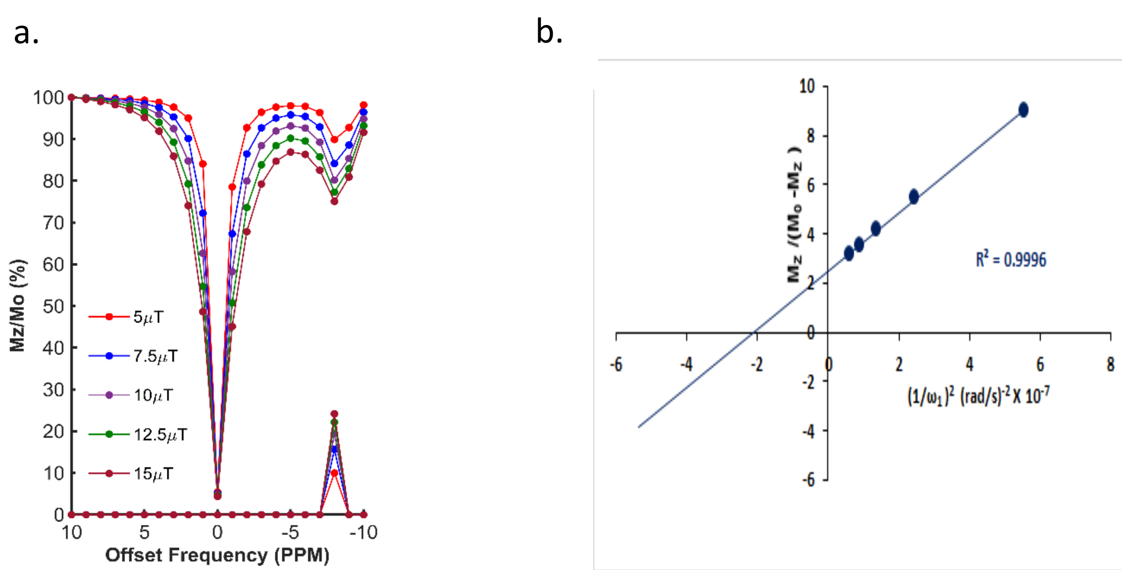

Figure S10: (a) Dependence of CEST percentage on saturation field strength ranging from 5μT to 15μT for pH 8.0 (b) Omega plot for exchange rate measurement. The expected linear relationship of $M_z/(M_0-M_z)$ as a function of $1/\omega_1^2$ (rad/sec)$^{-2}$ x 10^{-7} recorded at 9.4 T of 12.5 mM compound in 0.1M Tris-HCl buffer at pH 8.0. RF saturation pulse was applied for 6 s ensuring complete saturation.

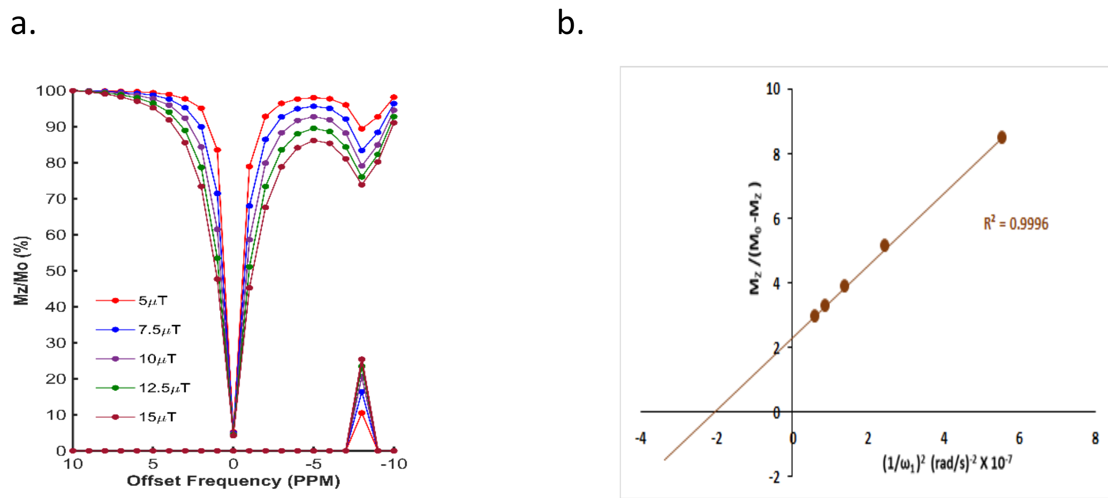

Figure S11 : (a) Dependence of CEST percentage on saturation field strength ranging from 5μT to 15μT for pH 8.3 (b) Omega plot for exchange rate measurement for pH 8.3. The expected linear relationship of $M_z/(M_0-M_z)$ as a function of $1/\omega_1^2$ $(rad/sec)^{-2}$ x 10^{-7} was obtained at 9.4 T of 12.5 mM compound in 0.1M Tris-HCl buffer. RF presaturation pulse was applied for 6 s ensuring complete saturation.

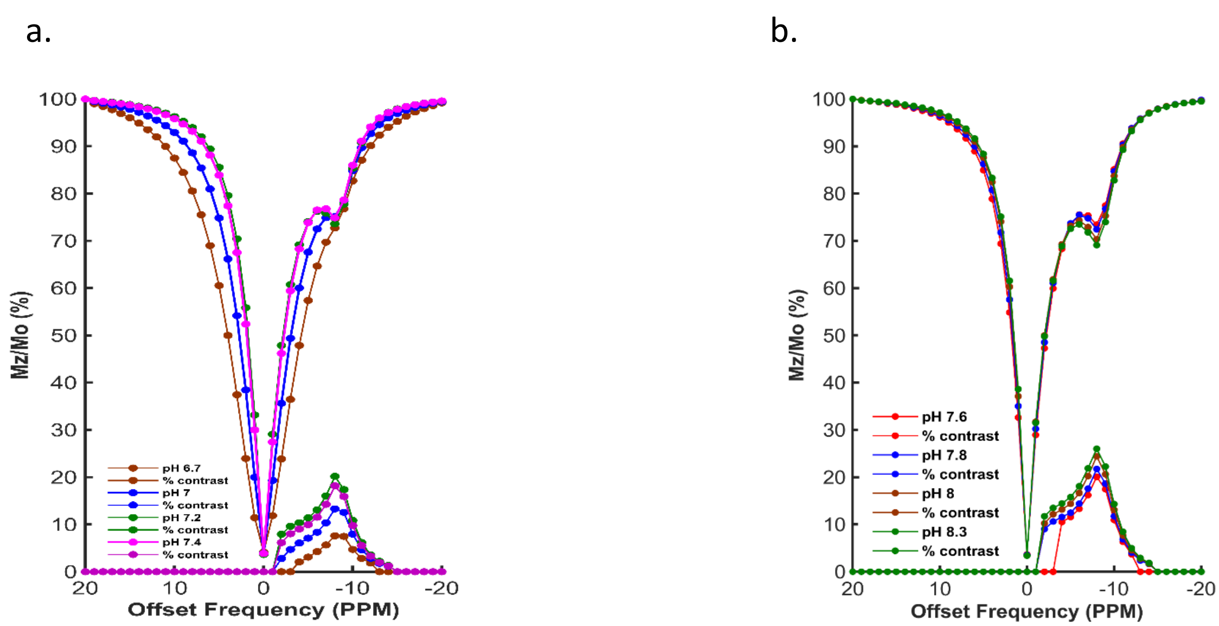

Figure S12 : Dependence of CEST effect of TmPyP on pH. (a) Overlaid Z-spectra with pH ranging from 6.7 to 7.4. (b) Overlaid Z-spectra with pH ranging from 7.6 to 8.3. Radiofrequency saturation was applied for 3s with a saturation radiofrequency of 5μT.

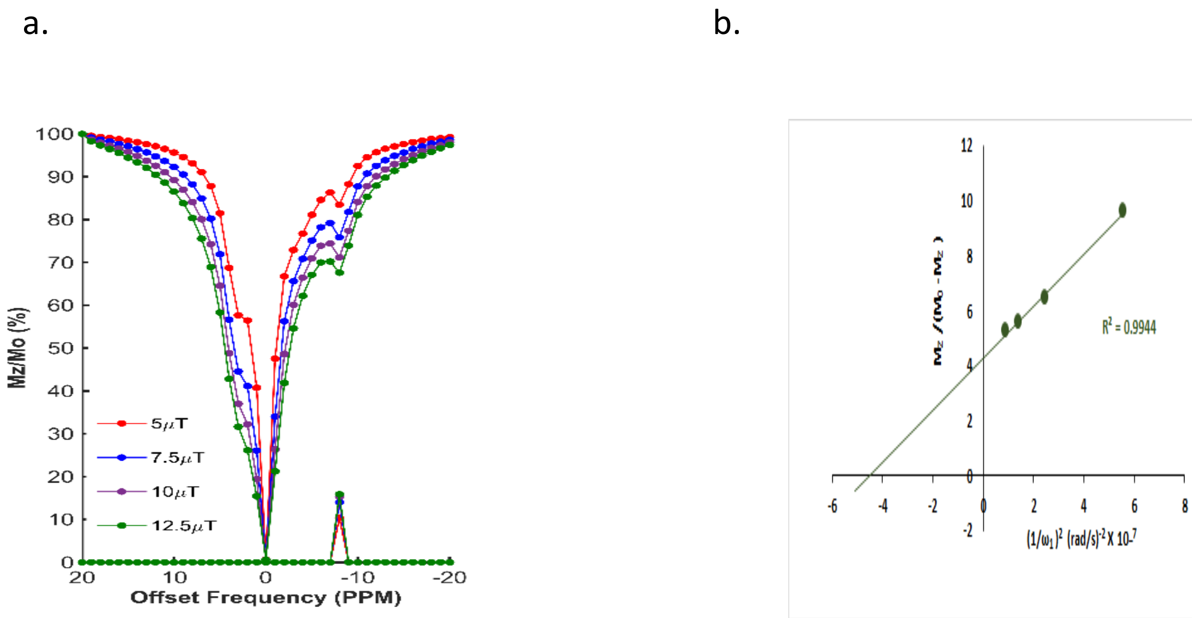

Figure S13 : (a) Dependence of CEST percentage on saturation field strength ranging from 5μT to 12.5μT for FBS at 7.4 pH (b) Omega plot for exchange rate measurement. The expected linear relationship of $M_z/(M_0-M_z)$ as a function of $1/\omega_1^2$ $(rad/sec)^{-2}$ x 10^{-7} recorded at 9.4 T of 12.5 mM TmPyP in Foetal bovine serum at pH 7.4. RF saturation pulse was applied for 6 s ensuring complete saturation.

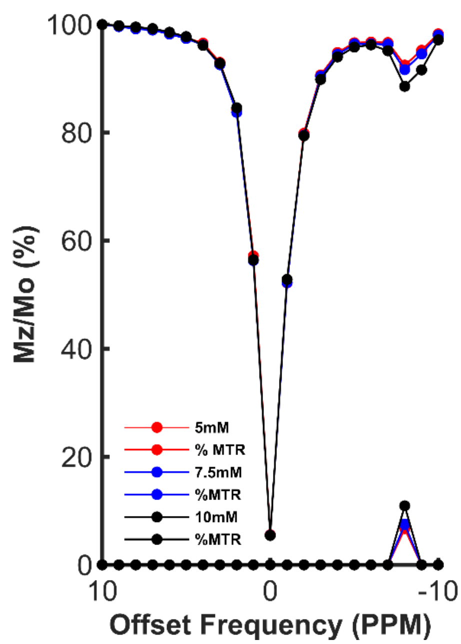

Figure S14: CEST contrast of **TmPyP** with varying concentration at pH 7.4 with a saturation field strength of 5μT. At 5 mM concentration **TmPyP** produced 6% CEST percentage.